Second harmonic generation and its interaction with relativistic plasma waves driven by forward Raman instability in underdense plasmas

V. Malka
Laboratoire pour l'Utilisation des Lasers Intenses, Centre National de la Recherche Scientifique, Ecole Polytechnique, 91128 Palaiseau Cedex, France

A. Modena, Z. Najmudin, and A. E. Dangor
Imperial College, London, United Kingdom

C. E. Clayton, K. A. Marsh, and C. Joshi
University of California at Los Angeles, Los Angeles, California 90024

C. Danson, D. Neely, and F. N. Walsh
Rutherford Appleton Laboratory, Chilton, United Kingdom

High conversion efficiency (0.1%) into second harmonic light generated in the interaction of a short-pulse intense laser with underdense plasma has been observed. In this experiment the plasma is created by optical field ionization of hydrogen or helium gas. Second harmonic spectra observed in the forward direction show Stokes and anti-Stokes satellites. This is due to the interaction of the second harmonic light with large-amplitude relativistic plasma waves. Second harmonic images taken at 30° from the propagation axis show that the radiation is generated over a length of a few times the Rayleigh length and that the origin of the second harmonic light is due to the radial electron density gradients created by the ionization process and the radial ponderomotive force. © *1997 American Institute of Physics.* [S1070-664X(97)02904-2]

I. INTRODUCTION

Harmonic generation has been a subject of great interest since the advent of high-intensity, short-pulse lasers. The highly nonlinear nature of the interaction of these laser pulses with gases and plasmas imply that harmonic light should be a significant feature of such interactions. Many mechanisms can generate laser harmonics in plasmas. In the case of the second harmonic, the main mechanism is the presence of density gradients in the plasma. Physically, this is due to the laser-induced quiver motion of the electrons across a density gradient, which gives rise to a perturbation δn in the electron density at the laser frequency ω_0 (as can be seen from the continuity equation). This density perturbation, coupled with the quiver motion of the electrons $v_{\rm osc}$, produces a source current J at the second harmonic frequency: $J = \delta n^* v_{\rm osc} \propto \cos^2(\omega_0 t) \propto \cos(2\omega_0 t)$. For electron density gradients transverse to the laser propagation direction, the currents are phased so as to radiate predominantly in the forward direction.

Second harmonic frequency generation has previously been observed using long laser pulses (300 ps) at intensity $<10^{15}$ W/cm^2 in a preformed underdense plasma in a direction perpendicular to the laser. This was attributed to ponderomotive self-focusing or filamentation of the high-intensity laser in a long scale length plasma.[1] Angularly resolved second harmonic measurements were reported in the interaction of a CO_2 laser with a nitrogen gas jet.[2] The forward second harmonic light was attributed to filamentation generation. CO_2 laser pulses[3] and Nd:glass laser pulses[4] interacting with helium gas-filled chambers also produced second harmonic light in the forward direction, again attributed to the production of filaments. In a more recent experiment,[5] the second harmonic of Raman sidescattered light was observed at 45° from the direct backscattered direction.

The interest in the interaction of intense laser pulses with plasma is not limited only to harmonic generation. The propagation of intense electromagnetic waves in an underdense plasma can also excite plasma waves via the forward Raman scattering instability (FRS).[6–8] This instability is of interest in laser inertial confinement fusion because it can generate energetic electrons that can preheat the fuel and reduce the implosion efficiency. Another case where FRS is of increasing interest is in laser particle acceleration. This is because it can excite a large-amplitude relativistic plasma wave that is therefore suitable for particle acceleration.[9–11] The interaction of a short-intense-laser pulse with an underdense plasma is also of interest in the ''fast ignitor'' fusion concept.[12] In this scheme, it is required to deliver a short, intense laser pulse to the (imploded) dense laser-fusion capsule. The intense pulse must propagate through a very long (few millimeter) region of underdense plasma and this propagation may be hampered by FRS.

In this paper we report on an experiment in which we observed FRS accompanied by second harmonic light generation with a conversion efficiency of up to 0.1%. Moreover, the second harmonic light was phase modulated by the copropagating relativistic electron plasma wave produced by FRS of the main laser beam. We also show explicitly that ionization-induced density gradients are one cause of second harmonic light and show that relativistic and/or ponderomotive self-focusing may be occurring, as evidenced by the observation of filamentary-shaped images produced by the second harmonic light emission.
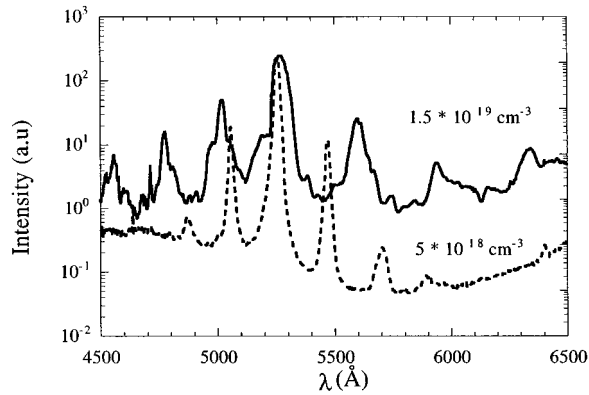
FIG. 1. Typical second harmonic forward spectra for an electron density of 1.5×10^{19} cm^{-3} (solid line) and 5×10^{18} cm^{-3} (dashed line). Laser power for both these shots was around 25 TW. The higher-density spectrum shows blue-shifted shoulders.

FIG. 2. Wavelength shift of the Stokes $(+)$ and anti-Stokes satellites $(-)$ as a function of the electron density. The reference numbers on each curve correspond to the satellite's number.

II. EXPERIMENTAL RESULTS

The experiment described here was performed at the Rutherford Appleton Laboratory[13] with the Vulcan Nd:glass laser operating at 1.054 μm in the chirped-pulse amplification (CPA) mode. In this configuration the laser provided 25 J in 0.7–1 ps pulses, which were focused, with an $f/4.5$ off-axis parabola, to a 20 μm diam spot. This corresponds to typical powers of 20–25 TW and to on-target intensities I_0 of the order of 5×10^{18} W/cm^2. The effective Rayleigh length (for a factor of 2 drop in laser intensity) was 350 μm. To avoid refraction induced by ionization processes,[3,14] the laser beam was focused onto the sharp edge of a 4 mm diam laminar plume of helium or hydrogen gas from a pulsed, supersonic gas jet[15] located 2 mm below the focal region. The typical focal intensity of 5×10^{18} W/cm^2 at $f/4.5$ is sufficient to fully optically ionize helium over at least 2 mm into the jet and hydrogen over the full 4 mm diam of the jet. The electron density in the gas jet was controlled by the density of neutrals that was varied by changing the backing pressure of the jet. The density was measured through the frequency shift $(n\omega_p)$ of the anti-Stokes sidebands of the pump laser, as created by FRS. The electron density was found to be linear with backing pressure from 5 to at least 18 bar, where the electron density was 1.5×10^{19} cm^{-3}. The two key diagnostics discussed in this paper are the forward scattered electromagnetic spectrum around the second harmonic frequency and images obtained at 30° from the direction of propagation of the laser taken through narrow band $2\omega_0$ interference filters.

The spectrum of the light transmitted in the forward direction was measured in the full $f/4.5$ cone angle of the incident laser. This light was transmitted through a pellicle that was antireflection coated at 1.054 μm so as to reject the pump laser beam. The spectrum was detected with a 16 bit silicon charge coupled device (CCD) camera. A bright blackbody source placed at the focal position of the pump laser was used to measure the overall transmission function of the optics and the spectral response of the CCD camera. This was used to correct the measured spectrum. Figure 1 shows the corrected spectra around the second harmonic wave-
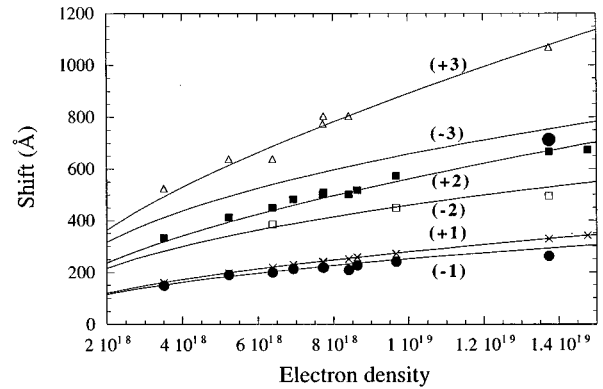
length 0.527 μm obtained for two different plasma densities: 5.4×10^{18} cm^{-3} (dashed curve) and 1.5×10^{19} cm^{-3} (solid curve). At low electron density, three Stokes satellites and two anti-Stokes satellites are clearly visible due to the interaction with a FRS-driven plasma wave. The positions of the peak of the satellites correspond to frequencies $2\omega_0 \pm n\omega_p$. In the high-density case the presence of three Stokes and three anti-Stokes satellites can be discerned. Here the displacement from the second harmonic wavelength is greater, consistent with a higher electron density. The satellites still correspond to frequencies of $2\omega_0 \pm n\omega_p$. The most remarkable feature is the broadening of the individual anti-Stokes peaks at this higher density. This is similar to the broadening observed in the incident transmitted laser spectrum, which, as discussed in a previous publication,[9] is characteristic of wave breaking of the plasma wave.

As mentioned by Krushelnick[5] in a experiment where the spectrum of the *backscattered* light was reported, two scenarios are possible for the generation of the Raman scattered satellites around the second harmonic: (i) laser light may be frequency-doubled passing the interaction region and scattered by the plasma wave, giving a cascade of satellites at $2\omega_0 \pm n\omega_p$; or (ii) the incident laser light is scattered by the plasma first, leading to a cascades of satellites at $\omega_0 \pm n\omega_p$ that are subsequently frequency doubled as they propagate, resulting in satellites at $2\omega_0 \pm 2n\omega_p$. Clearly, the presence of both the odd and even satellites of the second harmonic show that the first scenario is dominant in our forward-scattering experiment. In Fig. 2 we plot as a function of the electron density the shift of the Stokes $(+)$ and anti-Stokes satellites $(-)$. The reference number for each curve corresponds to the satellites number for example, the curve $(+2)$ corresponds to the theoretical wavelength shifts of the second Stokes satellites for a cold plasma, i.e. $2\omega_p$. To obtain the theoretical wavelength shifts one needs to know the effective electron density. As mentioned earlier, we acquire this effective electron density independently from the wavelength shifts of the first Stokes and anti-Stokes in the spectrum of the transmitted 1μm pump beam. Figure 2 shows that the experimental wavelength shifts are in good agreement with the theoretical value.

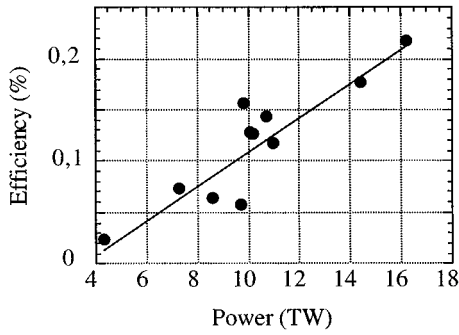In shots at higher electron densities, as can be observed

FIG. 3. Measured second harmonic efficiency as a function of the laser power.

3 millimeters

Laser

FIG. 4. Typical second harmonic image at 30° from the propagation axis in hydrogen.

in Fig. 1, a small amount of energy of the transmitted second harmonic (less than 10%) was slightly ($\approx$70 Å) blue-shifted. The blue-shift is a consequence of the time varying electron density due to tunnel ionization during the rising edge of the laser pulse:[16] the resulting variation in time of the refractive index self-modulates the phase of the laser during its propagation in the plasma. Its proper frequency is then increased, giving a blue-shift that is roughly proportional to the electron density. Similar but larger and more intense blue-shift features are obtained in the transmitted pump. The blue-shifting of the satellites of the second harmonic indicates that the onset of the second harmonic light (and its blue-shift) occurred during the ionization phase, early in time, and would thus precede the FRS, allowing the green light to interact with the relativistic plasma waves, as seen in Fig. 1.

III. DISCUSSION

In the experiment by Krushelnick et al.[5] ($I_0\approx2\times10^{18}$ W/cm^2 and $f/3$ focusing) no second harmonic light was observed in the forward direction in hydrogen and only a conversion efficiency of 10^{-6} was observed in helium. In contrast, we observed a high conversion efficiency for the generation of forward second harmonic light, about 10^{-3}, for both helium and hydrogen. The measured second harmonic conversion efficiency in the cone angle of the laser is plotted as a function of the laser intensity (changing the laser energy) in Fig. 3. This shows that the second harmonic conversion increases with laser intensity. A simple theoretical calculation for the conversion efficiency of second harmonic production due to interaction of a laser beam with density gradients is given by[5,17]

$$\eta=\frac{P_{2\omega_0}}{P_{\omega_0}}=\frac{a_0^2}{(1+a_0^2/2)}\left(\frac{L}{4L_\nabla}\frac{k_p^2}{k_0^2}\right)^2,$$

where $P_{2\omega0}$ (and $P_{\omega0}$) are, respectively, the power of the second harmonic and the pump laser, $a_0=eA/mc^2=0.86\times10^{-9}\lambda(\mu m)\sqrt{I_0(\mathrm{W/cm^2})}$ is the normalized vector potential of the laser, where λ is the laser wavelength and I is the laser intensity and k_0 (k_p) is the laser (plasma) wave number. L_∇ is the density gradient scale length and L is the interaction length. For our conditions L is limited by the detuning of the generated second harmonic from the pump laser due to dispersion in the plasma,[17] which is about 120
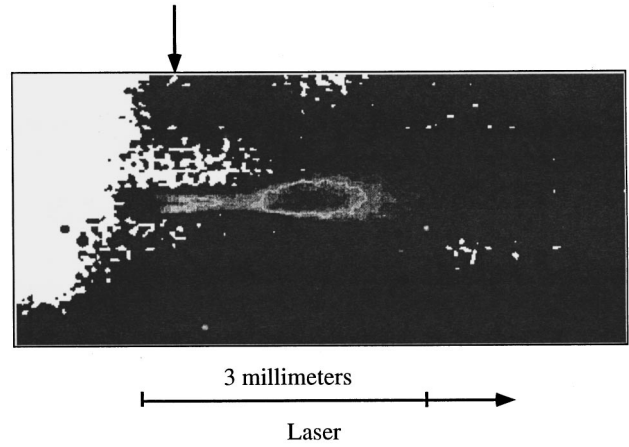
μm. L_∇ is taken to be around 10 μm, the focal spot radius. If we take $a_0=2$, which corresponds to our maximum intensity of 5×10^{18} W/cm^2 and a number density of 10^{19} cm^{-3}, we find an efficiency of 0.1%, which is of the order of the observed maximum efficiency. That the efficiency increases rather than saturating due to relativistic effects, as suggested by these simple treatments, can be attributed to enhancement of density gradients due to ponderomotive effects, which can occur at these higher intensities.

In Figs. 4 and 5 we present two typical second harmonics images obtained at 30° from the propagation direction (in the plane of the laser polarization) in hydrogen and helium, respectively. These images of the scattered second harmonic radiation from the interaction region were obtained using two $f/3$ achromatic lenses on a eight bit CCD camera with a depth of field of at least 4 mm. The spatial resolution was limited by the pixel size of the CCD to 20 μm. The second harmonic of the laser radiation was selected with a 10 nm full width at half-maximum (FWHM) interference filter centered at 0.53 μm. In order to be sure of the nature of the green light, we measured the full light spectrum at the same 30° angle. This spectrum exhibits an intense second harmonic component at 0.53 μm that completely dominates the
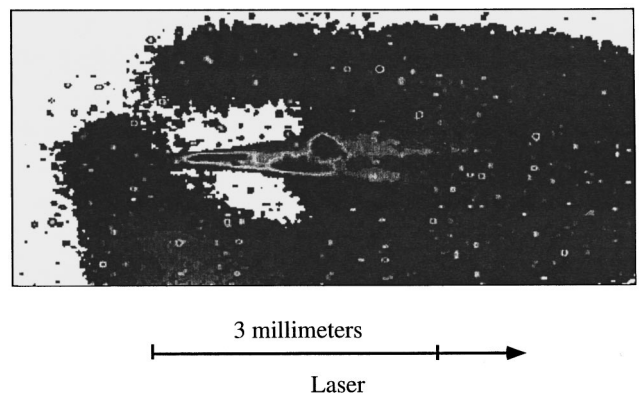

3 millimeters

Laser

FIG. 5. Typical second harmonic image at 30° from the propagation axis in helium. Small dots in the image are x-ray hits from accelerated electrons hitting the vacuum chamber.
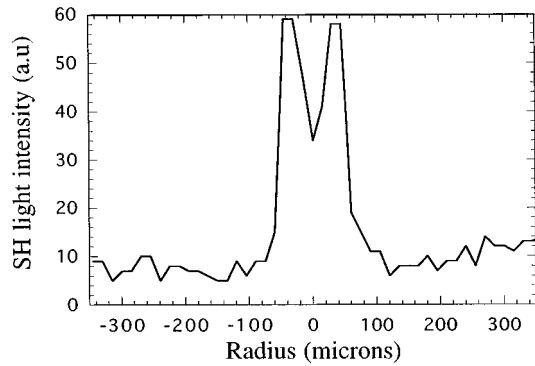
FIG. 6. Experimental radial second harmonic light profile obtained at the position defined by the arrow from the image in Fig. 3.
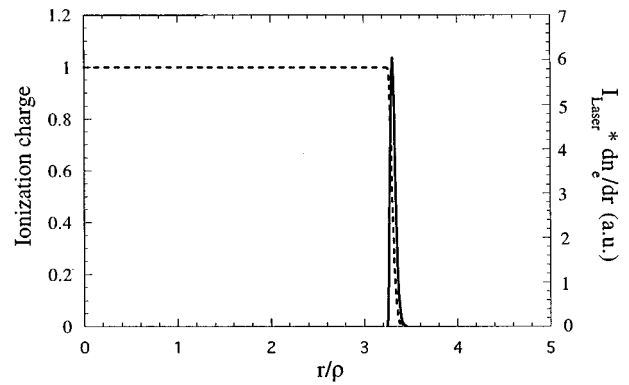

FIG. 7. Calculated radial electron density in the hydrogen case (dashed curve) and the product of the radial laser intensity with the radial electron density gradient (solid curve).

plasma recombination light in energy. We observe in these figures second harmonic light emanating over a distance of ≈ 3 mm, which is about eight Rayleigh lengths. Similar features were observed in the images taken at 1.053 μm. Enhanced longitudinal propagation lengths have previously been obtained in a similar experiment,[18] which imaged the scattered laser light (at ω_0) at 90°. In this experiment, by analyzing the axial intensity profile for different laser conditions, the authors concluded that relativistic self-channeling was responsible for the long images.

The images of the second harmonic light show signs of a single longitudinal filament. These filaments are much clearer in helium (Fig. 5) than in hydrogen (Fig. 4). In both types of plasma this structure appears more clearly when the gas pressure is higher. Since in this experiment the laser power is much greater than the critical power for relativistic self-focusing [$P_{cr}=17(\omega_p/\omega_0)^2$ GW], the laser can in theory self-channel, resulting in propagation of high-intensity filament of light[19] over a considerable distance. The laser intensity can be higher than its value in vacuum, due to the relativistic self-focusing. The transverse ponderomotive force associated with the optically guided laser pulse is then high enough to significantly expel the electrons from the laser axis, creating a sharp density gradient where second harmonic light can be generated. Hence the second harmonic filaments we see can be a signature of this self-channeling due to relativistic self-focusing. There is further evidence of this decrease in effective plasma density due to these relativistic/ponderomotive effects in the separation of the Raman sidebands as a function of intensity, as mentioned in a previous publication,[20] for it was found that the sideband separation for a constant backing pressure (and hence a constant initial density of neutrals), decreases with increasing intensity. This would be consistent with an effective decrease in plasma frequency due to relativistic quiver motion of the plasma electrons and/or a density depression due to ponderomotive blow-out. Recent experimental investigation using the same laser and plasma conditions have confirmed that relativistic laser intensities ($a_0 \approx 1$) are present in these filaments.[21]

Another interesting feature is evident in the hydrogen images in Fig. 4. At the beginning of the interaction region, a 100 μm before the focal plane, the radial second harmonic light intensity profile produces a minimum along the laser propagation axis. Figure 6 shows the radial intensity profile obtained at the position along the laser axis defined by the arrow in Fig. 4. The two maxima in the radial second harmonic light profile are separated by about 80 μm.

One can calculate the time-dependent electron density using the tunnel ionization rates[22] for hydrogen. Neglecting the effects of hydrodynamic motion for the duration of the laser, we can calculate the radial electron density at the position of peak laser intensity. The radial laser intensity profile is Gaussian, with a radius (to $1/e$) in intensity of 10 μm. In Fig. 7 we plot, on the same graph, the calculated electron density in hydrogen, and the product of the laser intensity with the electron density gradient, as a function of radial distance. This last quantity is the source term for the second harmonic light, as discussed earlier (see, for example, Ref. 19). This quantity present a maximum at 35 μm that is 3.5 $\times$the radius, giving two maxima about 70 μm apart. This compares favorably with the experimentally acquired value of 80 μs. We do not observe this feature in the helium case. This is probably due to the different ionization characteristics of the two gases. Helium is ionized at higher laser intensities, both for its first and second ionization. Consequently the density gradients due to ionization are less well defined for helium.

IV. CONCLUSION

In conclusion, we report here the first observation of the forward scattering of second harmonic ($2\omega_0$) light from relativistic electron plasma waves driven by FRS. The generation of the second harmonic light is consistent with the presence of radial electron density gradients resulting from both the ionization process and the radial ponderomotive force. The second harmonic conversion efficiency and its dependency on laser power agree well with theory. The bright second harmonic light scattered over a distance of several Rayleigh length indicates self-channeling.

Malka *et al.*

[1] J. A. Stamper, R. H. Lehmberg, A. Schmitt, M. J. Herbst, F. C. Young, J. H. Gardner, and S. P. Obenschain, Phys. Fluids **28**, 2563 (1985).

[2] J. Meyer and Y. Zhu, Phys. Fluids **30**, 890 (1987).

[3] W. P. Leemans, C. E. Clayton, W. B. Mori, K. A. Marsh, P. K. Kaw, A. Dyson, C. Joshi, and J. M. Wallace, Phys. Rev. A **46**, 1091 (1992).

[4] D. Batani, F. Bianconi, A. Giuletti, D. Giuletti, and L. Nocera, Opt. Commun. **70**, 38 (1989).

[5] K. Krushelnick, A. Ting, H. R. Burris, A. Fisher, C. Manka, and E. Esarey, Phys. Rev. Lett. **75**, 3681 (1995).

[6] D. W. Forslund, J. M. Kindel, and E. L. Lindman, Phys. Fluids **18**, 1002 (1975).

[7] C. Joshi, T. Tajima, J. M. Dawson, H. A. Baldis, and N. A. Ebrahim, Phys. Rev. Lett. **47**, 1285 (1981).

[8] W. B. Mori, C. D. Decker, D. E. Hinkel, and T. Katsouleas, Phys. Rev. Lett. **72**, 1482 (1994).

[9] A. Modena, Z. Najmudin, A. E. Dangor, C. E. Clayton, K. A. Marsh, C. Joshi, V. Malka, C. D. Darrow, C. Danson, D. Neely, and F. N. Walsh, Nature **377**, 606 (1995).

[10] K. Nakajima, D. Fisher, T. Kawakubo, H. Nakanishi, A. Ogata, Y. Kato, Y. Kitagawa, R. Kodama, K. Mima, H. Shiraga, K. Suzuki, K. Yamakawa, T. Zhang, Y. Sakawa, T. Shoji, Y. Nishida, N. Yugami, M. Downer, and T. Tajima, Phys. Rev. Lett. **74**, 4428 (1995); D. Umstadter, S.-Y. Chen, A. Maksimchuk, G. Mourou, and R. Wagner, Science **26**, 472 (1996).

[11] C. A. Coverdale, C. B. Darrow, C. D. Decker, W. B. Mori, K-C. Tzeng, K. A. Marsh, C. E. Clayton, and C. Joshi, Phys. Rev. Lett. **74**, 4659 (1995).

[12] M. Tabak, J. Hammer, M. E. Glinsky, W. L. Kruer, S. C. Wilks, J. Woodworth, E. M. Campbell, M. D. Perry, and R. J. Mason, Phys. Plasmas **1**, 1626 (1994).

[13] C. N. Danson, L. J. Barzanti, Z. Chang, A. E. Damerell, C. B. Edwards, S. Hancock, M. H. R. Hutchinson, M. H. Key, S. Luan, R. R. Mahadeo, I. P. Mercer, P. Norreys, D. A. Pepler, D. A. Rodkiss, I. N. Ross, M. A. Smith, R. A. Smith, P. Taday, W. T. Toner, K. W. M. Wigmore, T. B. Winstone, R. W. W. Wyatt, and F. Zhou, Opt. Commun. **103**, 392 (1993).

[14] P. Monot, T. Auguste, L. A. Lompré, G. Mainfrey, and C. Manus, J. Opt. Soc. Am. B **9**, 1579 (1992).

[15] R. Brückner, Ph.D. thesis, Université d'Orléans, 1994.

[16] W. M. Wood, C. W. Siders, and M. C. Downer, Phys. Rev. Lett. **67**, 3523 (1991).

[17] E. Esarey, A. Ting, P. Sprangle, D. Umstadter, and X. Liu, IEEE Trans. Plasma Sci. **PS-21**, 95 (1993).

[18] P. Monot, T. Auguste, P. Gibbon, F. Jakober, G. Mainfray, A. Dulieu, M. Louis-Jacquet, G. Malka, and J. L. Miquel, Phys. Rev. Lett. **74**, 2953 (1995).

[19] C. E. Max, J. Arons, and A. B. Langdon, Phys. Rev. Lett. **33**, 209 (1974).

[20] A. Modena, Z. Najmudin, A. E. Dangor, C. E. Clayton, K. A. Marsh, C. Joshi, V. Malka, C. D. Darrow, and C. Danson, IEEE Trans. Plasma Sci. **24**, 289 (1996).

[21] C. E. Clayton, P. Muggli, D. Gordon, K. A. Marsh, C. Joshi, V. Malka, Z. Najmudin, A. Modena, A. E. Dangor, D. Neely and C. Danson, ''Observation of self-channeling of relativistically-intense laser light in a plasma channel,'' submitted to Phys. Rev. Lett.

[22] M. V. Amnosov, N. B. Delone, and V. P. Krainov, Sov. Phys. JETP **64**, 1191 (1987).